

# AMCoR

Asahikawa Medical College Repository <http://amcor.asahikawa-med.ac.jp/>

Journal of Clinical Endocrinology and Metabolism (2004. Nov) 89  
(11):5851–5861.

Decreased expression of retinoid X receptor isoforms in human thyroid carcinomas

Takiyama, Yumi ; Miyokawa, Naoyuki ; Sugawara, Akira ;  
Kato, Shizuo ; Ito, Koichi ; Sato, Keisuke ; Oikawa,  
Kensuke ; Kobayashi, Hiroya ; Kimura, Shoji ; Tateno,  
Masatoshi

**Decreased Expression of Retinoid X Receptor (RXR) Isoforms**

**in Human Thyroid Carcinomas**

YUMI TAKIYAMA, NAOYUKI MIYOKAWA, AKIRA SUGAWARA, SHIZUO

KATO, KOICHI ITO, KEISUKE SATO, KENSUKE OIKAWA, HIROYA

KOBAYASHI, SHOJI KIMURA, AND MASATOSHI TATENO

The Second Department of Pathology (Y.T., K.T., K.O., H.K., M.T.), Surgical Pathology

(N.M., S. Kato) and School of Nursing (S. Kimura), School of Medicine, Asahikawa

Medical College, Asahikawa 070-8012; Department of Comprehensive Medicine (A.S.),

Tohoku University, Sendai 980-8578; Ito Hospital (K.I.), Tokyo 150-8308, Japan.

Abbreviated title: RXR Expression in Human Thyroid Cancer

Key words: RXR, Thyroid, Cancer

Present address (Y.T.): The Second Department of Internal Medicine, Asahikawa

Medical College

Address all correspondence and reprint requests to: Yumi Takiyama, M.D., Ph.D.,

The Second Department of Internal Medicine, Asahikawa Medical College,

Midorigaoka higashi 2-1-1-1, Asahikawa 078-8510, Japan.

E-mail address: [taka0716@asahikawa-med.ac.jp](mailto:taka0716@asahikawa-med.ac.jp)

## **Abstract**

Retinoid X receptors (RXRs) are ligand-inducible transcription factors that belong to the superfamily of nuclear hormone receptors. Because RXRs heterodimerize with thyroid hormone receptor, retinoic acid receptor, vitamin D<sub>3</sub> receptor, and peroxisome proliferator-activated receptor, they play central roles in regulating a number of signaling pathways. To understand the roles of RXRs in human thyroid carcinogenesis, we have investigated the immunohistochemical expression of RXRs in normal and neoplastic thyroid tissues. Whereas nontumorous human thyroid cells exhibited distinct nuclear staining for the RXRs, thyroid carcinomas showed decreased nuclear expression of all three RXR isoforms. Especially, some thyroid carcinoma cells showed intense RXR- $\alpha$  cytoplasmic staining accompanied by decreased immunoreactivity in their nuclei. This subcellular localization of RXR- $\alpha$  was confirmed by Western blot analysis, which showed both lower nuclear expression levels of RXR- $\alpha$  and a cytosolic presence of RXR-related protein in neoplastic regions. We present here for the first time the histological distribution of each RXR protein ( $\alpha$ ,  $\beta$ , and  $\gamma$ ) in human thyroid follicular cells. In addition, we found that the nuclear expression of RXRs was lower in thyroid

carcinomas than in normal tissue. The differential expressions of these RXRs in thyroid carcinomas might be implicated in the pathogenesis of thyroid cancers.

## **Introduction**

Retinoids regulate a broad range of biological processes, including growth, differentiation, and development. They have been administered in anticancer and preventive cancer treatments in various clinical trials (1-6). The biological actions of retinoic acid and its derivatives are mediated at the cellular level by two types of specific nuclear receptors: retinoic acid receptors (RARs) and retinoid X receptors (RXRs) (7). RXRs are ligand-inducible transcription factors belonging to the superfamily of nuclear hormone receptors, and they heterodimerize with thyroid hormone receptor (TR), retinoic acid receptor (RAR), vitamin D<sub>3</sub> receptor (VDR), peroxisome proliferator-activated receptor (PPAR), and with other, orphan receptors. RXRs thus play central roles in regulating a number of signaling pathways (7). Recent studies have reported the involvement of nuclear hormone receptors in thyroid carcinogenesis (8,9). Mutated TRs have been identified with significant frequency in papillary thyroid carcinomas (PTCs), suggesting that these TRs may be involved in the carcinogenesis of PTC (8). A PAX8-PPAR- $\gamma$  fusion gene was detected in 63% of follicular thyroid carcinomas (FTCs) but not in other thyroid tumors, indicating that this

fusion may be useful in the diagnosis and treatment of FTCs (9). As RXR is essential for the functioning of TRs and of PPAR- $\gamma$ , it could also contribute to behaviors specific to PTCs or FTCs. Moreover, functional RXRs have been reported in the human thyroid carcinoma cell lines and tissue samples, and the specific decreased expression of RXR- $\beta$  mRNA was observed in anaplastic thyroid carcinoma (ATC) cells as well as in human thyroid carcinoma samples (10). In most epithelial malignant cell systems, retinoids have been found to inhibit DNA synthesis. Hence, the reduced expression of RXRs in human thyroid tumors could conceivably interfere with retinoids' inhibition of DNA synthesis, and could thus contribute to the development of thyroid carcinomas.

We therefore hypothesize that abnormal expression of RXRs is also a critical step in human carcinogenesis, and that retinoids' therapeutic effects in thyroid cancer may be mediated through the normalization or enhancement of the RXRs' biological functions. The aims of the current study were to determine which RXR isoforms are present in thyroid carcinomas and to evaluate the expression of each RXR in order to determine whether or not differences in that expression in thyroid carcinomas could contribute to thyroid carcinogenesis.

## **Materials and Methods**

### ***Tissue samples***

Samples of pathologic human thyroid tissue were resected from patients whose thyroid carcinomas had been surgically removed. As a control, normal tissue counterparts of thyroid tumors were excised. The samples were immediately snap-frozen in liquid nitrogen after surgical removal and stored at  $-70^{\circ}\text{C}$  until use. The surgical tissue samples were obtained with the informed consent of the patients according to the regulations of the local ethics committee.

### ***RXR antibodies***

Two polyclonal antibodies against human RXR- $\alpha$  (D-20 and  $\Delta$ DN197) were purchased from Santa Cruz Biotechnology (Santa Cruz, CA, USA). The epitopes recognized by one of the anti-RXR- $\alpha$  antibodies (D-20) were residues 2-21, and those recognized by the other antibody ( $\Delta$  DN197) were residues 198-462. Polyclonal antibodies against RXR- $\beta$  and RXR- $\gamma$  were raised against synthetic peptides containing the following mouse RXR amino acid residues: RXR- $\beta$ , 78-93; RXR- $\gamma$ , 35-54 (11). The amino acid

sequences of mouse RXRs used as immunogens to construct these antibodies bear 100% homology with the human RXR- $\gamma$  sequence and 83% (three amino acid differences) with the human RXR- $\beta$  isoform. The characterization of these RXR antibodies was confirmed by Western blotting and immunoprecipitation as described previously (11).

### ***Immunohistochemistry***

In this study, we examined RXR expression in 176 thyroid carcinomas (57 papillary thyroid carcinomas (PTC), 40 follicular thyroid carcinomas (FTC), 24 anaplastic carcinomas (ATC), 28 medullary carcinomas (MTC), and 27 follicular adenomas (FA)). Formalin-fixed sections of normal thyroid and carcinoma were deparaffinized and incubated with 1% hydrogen peroxide in methanol for 30 min to block endogenous peroxidase activity, and then were microwaved at 100 °C for 15 min to retrieve antigenicity. Then the specimens were incubated overnight with the primary antibodies, rinsed in PBS, and subsequently incubated with ENVISION+ (DAKO, Carpinteria, CA) for 30 min. The reactions were visualized with 3, 3'-diaminobenzidine

tetrahydrochloride (DAB) after 2-3 min, revealing brown staining. The cell nuclei were then counterstained with hematoxylin. In the present study, we performed immunohistochemical preabsorption tests to confirm the specificity of the immunohistochemical reaction by preincubating the diluted antibodies with the corresponding antigen overnight at 4 °C prior to the immunohistochemical procedure. The immunoreactivity of each RXR was evaluated independently by two of the authors (Y.T., and M.T). The intensity of staining was classified separately for the nucleus and the cytoplasm, and was evaluated on a scale of 0-3 (0 and 3 corresponded to the absence and highest degree of staining, respectively). These independent assessments [between authors] did not differ by more than one scale level. As normal follicular thyroid cells showed moderate (2) or strong (3) nuclear staining with absent (0) or weak (1) cytoplasmic staining, a tumor was considered to have a suppressed nuclear RXR expression when the nuclear intensity level of the tumor cell was below 2 (moderate); if the cytoplasmic staining level was higher than 2, a tumor was considered to have increased cytoplasmic RXR expression.

### ***Cell Culture***

Three carcinoma cell lines—thyroid papillary NPA, follicular WRO, and anaplastic ARO—were kindly donated by Dr. Yuji Nagayama, University of Nagasaki (Nagasaki, Japan). These cells were cultured in RPMI-1640 medium (Gibco Oriental Co., Ltd., Tokyo, Japan) containing 10% heat-inactivated fetal calf serum (FCS) (Gibco) and antibiotics (100 IU/ml penicillin, 100 µg/ml streptomycin) in 5% CO<sub>2</sub> and at 95% humidity. The culture medium was changed every 3-4 days, and cells were passaged every 5-6 days.

### ***Reverse-Transcriptase (RT) PCR***

Total RNA was extracted from human thyroid whole tissue and thyroid cancer cell lines by homogenization using Sepasol-RNA I (Nacalai Tesque, Inc., Kyoto, Japan), according to the manufacturer's protocol. The samples obtained were quantified by absorbance at 260 nm. cDNA was synthesized using an A-MuLV reverse transcriptase (AMV-RT) in a 20-µl reaction containing 1.6 µg oligo-p(dT)<sub>15</sub> primer, 50 units RNase inhibitor, 1 mM each of dNTP, 2 µl 10 x reaction buffer, 5 mM MgCl<sub>2</sub>, 20 units

AMV-RT (all from Roche Diagnostics Corp., Indianapolis, IN), and 2 µg of total RNA. The reactions were incubated at 25 °C for 10 min, 42 °C for 60 min, 99 °C for 55 min, and finally cooled to 4 °C. cDNA was amplified using the Expand™ High Fidelity PCR System (Roche) in 25 µl of the final volume, which was one-fifth of the RT products, 10 pmol each of the sense and antisense primers, and 1.75 units of Taq DNA polymerase. The oligonucleotide primers for RT-PCR were designed using the published sequence of each target gene. The primers and conditions used, as well as the expected sizes from the reported cDNA sequences, are shown in Table 1. To examine the presence of splicing variants, the sequences of the RXR-α primer pairs were as follows: a forward primer (5'-CAGACATGGACACCAAACAT-3', nucleotide position: 64-83) and a reverse primer (5'-CCGCAGGCCTAAGTCATTTG-3', nucleotide position: 1465-1446). The numbers of PCR cycles were determined to amplify the products logarithmically. After the PCR products were visualized on 2% agarose gel stained with ethidium bromide, the amplified PCR products were excised from the gel and subcloned into TA cloning vectors (Invitrogen Co., Carlsbad, CA). Inserts were sequenced by an automatic DNA sequencer (Perkin-Elmer Cetus, Norwalk, CT).

### ***Relative quantification of mRNAs of human RXR isoforms***

The expression of each RXR isoform's mRNA in tissues was analyzed by two-step real-time RT-PCR using LightCycler-DNA Master SYBR Green I (Roche) as described previously (12).  $\beta$ -actin was used as the reference gene for the tissue examination. The same primers for RXR- $\alpha$ , - $\beta$ , - $\gamma$  and  $\beta$ -actin were used for the conservative RT-PCR (Table 1). For quantification, an external calibration curve was used. The RXR isoforms and the  $\beta$ -actin PCR products amplified by each primer pair were cloned separately in pCR2.1 vector (Invitrogen). For each plasmid, a dilution containing from  $10^3$  to  $10^9$  dsDNA molecules was used as a standard template for the production of an external calibration curve. The LightCycler instrument (Roche) was used to optimize the RT-PCR conditions for the  $MgCl_2$  concentrations, annealing temperatures, elongation time, and fluorescence acquisition temperature. PCR amplifications were performed in triplicate. The PCR efficiencies (E) were calculated according to the equation  $E=10^{-1/\text{slope}}$ . Each mean slope of each external calibration curve was used as a representative slope value. The CP (crossing point) for each transcript was determined

by the “fit point method” performed in the LightCycler software ver. 3.3 (Roche). The average triplicate CP value for each transcript was used as the representative CP value.

The relative quantification ratio of each thyroid tissue sample was calculated according to the following equation:  $\text{ratio} = (E_{\text{target}})^{\Delta\text{CP}_{\text{target}}(\text{control-sample})} / (E_{\text{ref}})^{\Delta\text{CP}_{\text{ref}}(\text{control-sample})}$ .  $E_{\text{target}}$  indicates the PCR efficiency when an RXR isoform’s primers and its standard template were used.  $E_{\text{ref}}$  refers to the PCR efficiency when the reference gene ( $\beta$ -actin) primer pairs and standard template were used.  $\Delta\text{CP}_{\text{target}}(\text{control-sample})$  and  $\Delta\text{CP}_{\text{ref}}(\text{control-sample})$  refer to the CP deviation of each thyroid carcinoma versus a control normal thyroid tissue (normal thyroid tissue paired with PTC 1) for each RXR isoform transcript and reference gene transcript, respectively (13).

### ***Extract preparation***

Protein extracts were prepared using a standard method described previously, with minor modifications (14). Briefly, human thyroid tissues were homogenized in 1 ml phosphate-buffered saline (PBS) with the Complete, Mini, EDTA-Free protease inhibitor cocktail (Roche). Cultured cells were washed with medium without serum and

twice with PBS, and were collected using a cell scraper. The scraped cells or homogenates were then centrifuged at 1000 g for 10 min at 4 °C. The pellets were washed with PBS containing the protease inhibitors mentioned above and were resuspended in 1~2 volumes of prechilled hypotonic buffer A (10 mM Hepes at pH 7.9, 10 mM KCl, 1.5 mM MgCl<sub>2</sub>, 0.5 mM dithiothreitol, protease inhibitor cocktail). After the suspension sat for 10 min on ice, 0.1 vol of 10% Nonidet P-40 was added to it, and the cells were lysed by vortexing. After centrifugation at 15000 rpm for 30 s, the supernatant obtained was collected as the cytoplasmic fraction. Soluble nuclear extracts were prepared by resuspending the pellet in an equal volume of prechilled hypertonic buffer C (20 mM Hepes at pH 7.9, 0.42 M NaCl, 1.5 mM MgCl<sub>2</sub>, 0.2 mM EDTA, 25% glycerol, 0.5 mM dithiothreitol, protease inhibitor cocktail), followed by incubation on ice for 30 min. After centrifugation at 13000 rpm for 10 min, the supernatant collected constituted the nuclear extract.

***Western blot analysis of RXR isoforms.***

The samples (standardized to 20 µg of total protein per lane) were mixed with the same

volume of 2x loading buffer containing 2% SDS and 10% of  $\beta$ -mercaptoethanol. They were then boiled for 5 min and analyzed on 4-12% NuPage bis-Tris SDS-PAGE gels (Invitrogen). After each gel was soaked in transfer buffer (glycine 33.3 mM, Tris 48 mM, SDS 1.3 mM, methanol 20% v/v), it was blotted onto an Immobilon-P membrane (Millipore, Bedford, MA) at 100 mA for 1 hr. The blot was saturated overnight at 4 °C in phosphate-buffered saline (PBS) and 0.1% Tween 20 (PBS-T buffer) containing 5% nonfat dry milk, washed twice in PBS-T for 10 min at room temperature, and then incubated with each of the rabbit anti-human RXR isoforms overnight. After the blot was washed three times in PBS-T (each wash lasted 10 min), the blot was stained with a 1:2,000 dilution of peroxidase-conjugated anti-rabbit IgG antiserum (Amersham Pharmacia Biotech, Little Chalfont, UK) for 1 hr at room temperature, and then was washed again five times for 10 min each time in PBS-T. Bands were visualized by the enhanced chemiluminescence (ECL) system according to the manufacturer's instructions (Amersham).

### *Statistical analysis*

The Friedman test was used to analyze differences in the expression levels of nuclear or cytoplasmic RXRs among different thyroid tumor histologic types. The statistical differences in expression among the RXRs were compared in two groups of neoplasms using Tukey's test post hoc. For comparative analysis, the two-tailed Fisher's exact test was used to compare the differences in the expression of the RXR isoforms between the histologic types. A p value of  $<0.05$  was accepted as statistically significant.

## Results

### *Immunohistochemical detection of RXR proteins in the human thyroid follicular cells*

To investigate a potential association between RXR expression and thyroid carcinogenesis, we first analyzed the expression of each RXR isoform in 57 PTC, 40 FTC, 24 ATC, 28 MTC, and 27 FA by immunohistochemistry. The upper half of Fig. 1 demonstrates the results of this analysis. The lower half shows the results of Western blotting of nuclear or cytoplasmic protein preparations of a papillary thyroid carcinoma and matched normal thyroid tissue. Each RXR isoform is represented by appropriately sized protein bands in the nuclear extracts from the normal thyroid tissues (Fig. 1 bottom, lane 1, arrow). The two immunoreactive bands in the nuclear extracts from the normal thyroid tissue are detected by the anti-RXR- $\gamma$  antibody (Fig. 1 right panel). The lower band (~50 kDa) corresponds to the form previously reported by Sugawara *et al.* (11), while the upper band (Fig. 1 bottom, arrow head) has been considered to represent a different phosphorylation state, an alternate form of RXR- $\gamma$ , or a protein that cross-reacts with the RXR- $\gamma$  antiserum (15). The nuclear extracts from PTC, which showed no nuclear staining for any of the RXR isoforms in immunohistochemical

analysis (Fig. 1, top panel, arrow head), were negative in the Western blots (Fig. 1 lane 2). The cytoplasmic extract from PTC, which showed strong cytoplasmic immunostaining for RXR- $\alpha$  (Fig. 1, top right panel), reacted strongly at a molecular mass of approximately 44 kDa to the anti-RXR- $\alpha$  antibody (D-20) (Fig. 1 asterisk).

The RXR isoforms were readily detected in all thyroid tumors and surrounding normal thyroid tissues. These immunostainings were abolished when blocking peptides were added to the diluted antibodies for each RXR isoform (Fig. 2 B, D, F). Normal follicular thyroid cells showed diffuse strong (3) to moderate (2) nuclear signals, whereas cytoplasmic staining was almost absent (Fig. 2 A, C, E). Homogeneous staining in the nucleus was seen at a higher magnification (Fig. 2 E insert). The intensity of immunostaining by the RXR isoforms in the nuclei and cytoplasm of thyroid tumors was relatively uniform within each specimen. Due to differences in the affinities of the antibodies, it is not possible to draw conclusions about the relative expression levels of the three isoforms. However, these levels differed among the isoforms in normal thyroid tissues and thyroid carcinomas. We observed a tendency toward suppression of the RXRs' nuclear expression in thyroid tumor cells

relative to that in adjacent normal thyroid follicular cells (Fig. 2 A, E). Unexpectedly, in addition to nuclear staining, a strong granular cytoplasmic staining was observed in some thyroid carcinomas by the anti-RXR- $\alpha$  antibody (D-20) (Fig. 2A, insert); this staining was abolished by peptide preabsorption (Fig. 2B). In contrast with the PTCs, the FTCs showed higher levels of nuclear immunostaining of the RXR- $\alpha$  protein. Therefore, RXR- $\alpha$  indicated distinct nuclear staining without cytoplasmic staining in the FTCs (data not shown). Occasionally, the ATCs showed weak or absent nuclear staining of RXR- $\alpha$ , as evidenced by a mild granular cytoplasmic staining (Fig. 2G). Only the cytoplasmic distribution of RXR- $\alpha$  protein shown in the PTCs was observed in the MTCs; that is, neither RXR- $\beta$  nor - $\gamma$  was detected in the nucleus or cytoplasm of the MTCs (Fig. 2E). Moreover, none of the RXR isoforms was detected in normal C-cells by immunohistochemistry (data not shown). In contrast to the results obtained with thyroid carcinomas, the RXR- $\alpha$  (Fig. 2 H) and - $\beta$  nuclear staining of benign follicular adenoma (FA) specimens was moderate, and similar to that of normal follicular thyroid cells in the same section (data not shown).

Immunohistochemical evaluation of the RXR isoforms' expression patterns

are also summarized in Table 2. Most PTCs (42 of 57) showed decreased levels of nuclear expression, accompanied by moderate or strong cytoplasmic expression for RXR- $\alpha$ . However, as seen in Table 2, some PTCs (4 of 57) indicated moderate or strong nuclear staining accompanied by moderate or strong intensities of cytoplasmic staining. Similarly, FTCs showing decreased levels of nuclear expression (21 of 40) mostly were accompanied by moderate or strong cytoplasmic staining (17 of 40) for RXR $\alpha$ . Compared with PTCs, a greater proportion of FTCs (19 of 40) showed moderate or strong nuclear immunostaining for RXR- $\alpha$ . None of the ATCs indicated moderate or strong nuclear expression for RXR- $\gamma$ . In contrast to the carcinomas, FA showed distinct nuclear immunostaining for RXR- $\alpha$  and - $\beta$ . The relationship between the expression of each RXR isoform and the tumor type was analyzed by the Friedman test. The nuclear and cytoplasmic expression values of the isoforms were significantly decreased in all four classes of thyroid carcinomas ( $p < 0.05$ ), except for the cytoplasmic expression of RXR- $\alpha$  protein ( $p = 0.27$ ). However, there was only a specific correlation between nuclear RXR- $\gamma$  expression and histological typing of thyroid tumors ( $p = 0.04$ ), indicating a statistical difference between PTC and ATC in the nuclear expression of RXR- $\gamma$

( $p < 0.05$ ).

Because normal follicular thyroid cells showed moderate (level=2) or strong (level=3) nuclear staining accompanied by absent (level=0) or weak (level=1) cytoplasmic staining, a tumor was considered to have a suppressed nuclear RXR expression when the nuclear intensity level of the tumor cell was lower than 2 (moderate); if the cytoplasmic staining level was higher than 2, a tumor was considered to have an increased cytoplasmic RXR expression. The intensity of staining was compared to that of normal thyroid follicular cells in the margin of each specimen. Figure 3 summarizes the results of this investigation. The nuclear RXR- $\alpha$  immunostaining was substantially suppressed in PTCs (80.7%) and FTCs (52.5%; Fig. 3). Statistically, RXR- $\alpha$  nuclear suppression in PTCs was significantly greater than in FTCs ( $p=0.004$ ), whereas the cytoplasmic RXR- $\alpha$  immunostaining was profoundly greater in PTCs than in FTCs ( $p=0.024$ ; Fig. 3). Although all three RXR isotypes were suppressed in PTCs and FTCs, there was no statistically significant difference in RXR- $\beta$  or RXR- $\gamma$  expression between PTCs and FTCs. The percentage of positively stained (staining level of 2 or 3) FTC nuclei was higher than that of positively stained

PTC nuclei in RXR- $\alpha$ (FTC vs. PTC, 47.5% vs.19.3%) and in RXR- $\beta$  (FTC vs. PTC, 35% vs.15.8%). However, the percentage of nuclei with positive RXR- $\gamma$  nuclear expression was divergent from the percentages for the other two RXR isoforms (FTC vs. PTC, 27.5% vs. 38.6%). A similarly low percentage of positively stained RXR- $\gamma$  nuclei was also obtained on benign FA. The only other statistically significant difference among expression levels of the RXR isoforms between FTC and FA was in nuclear RXR- $\beta$  staining. MTC, which were derived from C-cell and which did not show the positive immunostaining for each RXR isoforms, had the significant suppression of nuclear expressions for RXR $\alpha$ , for RXR $\beta$ , and for RXR $\gamma$  compared with other thyroid tumors(except ATC).

The nuclear RXR expression levels seemed to vary according to the extent of differentiation. The percentages of nuclei with suppressed nuclear expression of RXR isoforms were significantly higher in ATCs than in benign FA ( $p < 0.05$ ). Furthermore, in general, the ATC specimens had much lower nuclear RXR- $\alpha$  or - $\gamma$  expression levels than did specimens of highly differentiated thyroid carcinomas (PTCs and FTCs).

### ***mRNA expression of RXR isoforms in PTCs, FTC, MTC, and FA***

Next, we examined the gene expression levels of the RXR isoforms in human thyroid tumors. First, we evaluated the possibility that PTC showing cytoplasmic immunostaining for RXR- $\alpha$  protein would also express different sizes of mRNA; for this, we used primers for the complete mRNA of RXR- $\alpha$  (Fig. 4 A). Identically sized fragments were obtained for both PTC and normal thyroid tissue (Fig. 4A). We then examined the quantitative measures of mRNA expression of the RXR isoforms in thyroid tumors and normal thyroid tissue using real-time RT-PCR. Before this step, though, to discriminate the amounts of contaminated DNA in the RNA samples, we performed conservative RT-PCR without AMV reverse transcriptase, and then we confirmed the negative bands seen in the negative controls (data not shown). Using the LightCycler, we performed two-step real-time RT-PCR for 6 PTCs, one FTC, one MTC, and one FA (Fig. 4B). The RXR isoforms were differentially expressed in all nine normal thyroid tissues, but expression was lower in five (for RXR- $\alpha$  or - $\beta$ ) of six PTCs, in FTC, and in benign FA when compared with matched normal tissue. One tumor tissue (PTC 4, Fig.4B) showed higher expression of all three RXR isoforms. Another tumor

tissue (PTC 5, Fig.4B). indicated higher expression of RXR- $\gamma$ . For all of the isoforms, there were no significant differences in gene expression between normal thyroid tissue and neoplastic lesions. The mRNAs of all the isoforms were detected in all specimens, even in the thyroid carcinomas in which nuclear immunostaining for RXR isoforms was absent (data not shown). Therefore, the reduction in the expression of RXR isoforms observed at the protein level in thyroid carcinomas was not associated with a reduction in all mRNAs encoding the three receptors.

#### ***Western blotting of RXR- $\alpha$ in PTCs.***

To confirm the immunohistochemical cytoplasmic RXR protein expression in PTCs, we also performed Western blot analysis of PTCs. Identical results were obtained when CEs and NEs of PTCs were fractionated and subjected to Western blotting (Fig. 5B). The results in Fig. 5B show the presence of a 54-kDa protein species corresponding to the predicted size of RXR- $\alpha$  in NEs from the normal surrounding tissues. The NEs from tumor tissues, which showed absent or weak nuclear staining for RXR- $\alpha$  in immunohistochemical analysis, were weaker than those from normal tissues

in Western blots (Fig. 5B). In CEs from all tumor specimens, anti-RXR- $\alpha$  antibody (D-20) stained proteins with molecular masses of approximately 47, 44, and 40 kDa, whereas marginal reactions were observed in CEs from normal thyroid cells (Fig. 5B).

#### ***Western blot analysis using two specific RXR- $\alpha$ antibodies***

Previous studies have reported that the RXR- $\alpha$  molecule gets truncated as a result of degradation (16-18). To evaluate the possible existence of a truncated RXR- $\alpha$  protein, we performed Western blotting of NEs and CEs from PTC using two specific RXR- $\alpha$  antibodies (Fig. 5A). An RXR- $\alpha$ -related protein with an apparent molecular mass in SDS-PAGE of approximately 44 kDa was observed by immunoblotting analysis using the specific RXR- $\alpha$  antibody raised against sequences in the NH<sub>2</sub> terminus of human RXR- $\alpha$  (D-20; Fig. 5C, asterisk). However, Western blotting performed with an antibody raised against the complete ligand binding domain (E domain) of human RXR- $\alpha$  ( $\Delta$ DN197) failed to detect the 44-kDa protein (Fig. 5C). Furthermore, to examine the subcellular expression of RXR- $\alpha$  protein in FTC and MTC, we performed Western blot analysis of FTCs and MTCs with two different histological types, each

showing absent (level=0; FTC<sub>1</sub> and MTC<sub>1</sub>, Fig.5D) or moderate to strong (level= 2 to 3; FTC<sub>2</sub> and MTC<sub>2</sub>, Fig.5D) cytoplasmic RXR- $\alpha$  expression. The immunohistochemical data were supported by Western blot analysis. The RXR- $\alpha$ -specific 54-kDa band in NE from normal thyroid tissues was darker than the band from MTCs (Fig. 5D, *arrowhead*). One FTC tumor with distinct nuclear RXR- $\alpha$  staining (FTC<sub>1</sub>, Fig.5D) showed stronger immunoreactivity toward the 54-kDa protein than did the normal thyroid tissue. Immunoreactive protein was also detected at 44 kDa with the RXR- $\alpha$  (D-20) antibody, but it was not detected by another RXR- $\alpha$  antibody ( $\Delta$ DN197), in the CE from two specimens (MTC<sub>2</sub> and FTC<sub>2</sub>, Fig. 5D, *asterisk*).

### ***Expression of RXR in thyroid carcinoma cell lines***

Finally, we evaluated the expression levels of the RXR isoforms' mRNAs in three human thyroid cancer cell lines, ARO, WRO, and NPA. Figure 6A shows that, although RXR- $\alpha$  and RXR- $\beta$  mRNAs were detected under basal conditions in all cell lines, RXR- $\gamma$  transcript was expressed in NPA and ARO but was undetectable in WRO, the FTC cell line. We also performed Western blot analysis of NE and CE protein

extracts from human thyroid cancer cell lines. Figure 6B shows that the RXR- $\alpha$  protein (54 kDa) was present in NE, while approximately 44-kDa immunoreactive bands were seen in CE from all three cell lines. In contrast to the immunohistochemical findings for human thyroid carcinomas, nuclear RXR- $\alpha$  protein was expressed abundantly in ARO but only slightly in WRO cells.

## Discussion

In the present study, we examined the distribution of RXR isoforms in the normal human thyroid and in thyroid carcinomas, and identified a marked difference in receptor expression between these isoforms. Previous studies have shown that RXR- $\alpha$  and RXR- $\beta$ mRNAs are widely expressed (19-22), whereas the expression of RXR- $\gamma$  mRNA is restricted to tissues such as those in skeletal muscle, heart, brain (21,22), hypothalamus (23,24), and pituitary (11, 15, 23, 25-27). Dolle *et al.* (23) first demonstrated the diffuse expression of RXR- $\gamma$  transcript in the murine thyroid gland. Very recently, two studies from separate laboratories demonstrated the localization of RXR- $\gamma$  transcripts in normal human thyroid tissues (28) and thyroid tumors (28, 29). Consistent with these two studies, our present data first confirmed the presence of RXR- $\gamma$  protein in normal and neoplastic human thyroid follicular cells (Fig. 1 and Fig. 2, E and F). These findings were extended by demonstrating the expression of the RXR isoforms *in vitro*. The mRNA of both RXR- $\alpha$  and RXR- $\beta$  were found to be expressed in all three human thyroid cancer cell lines (ARO, WRO, and NPA; Fig. 6A). Interestingly, WRO cells derived from the FTC cell line did not express RXR- $\gamma$  mRNA

(Fig. 6A). Our results agree with the recent data described by Haugen *et al.* (29), which indicated the complete absence of RXR- $\gamma$  protein expression in WRO cells. These cell lines also exhibited the cytoplasmic RXR- $\alpha$  protein shown in the human thyroid tissue samples (Fig. 6B). The differential RXR expression in these thyroid cancer cell lines may be a useful model with which to investigate the mechanisms underlying the translocation and degradation of RXR- $\alpha$  in human thyroid carcinomas, as well as the correlation between retinoic acid-induced response and expression of the RXRs.

This study reveals that the nuclear expression of RXR isoforms was decreased in human thyroid tumors (Fig. 3, Table 2). One previous report has shown a marked decreased or absent expression of RXR- $\beta$  mRNA in nine of 12 human thyroid carcinoma samples examined (three FTCs, three oncocytic carcinomas, and six PTCs), suggesting a possible role for RXR- $\beta$  in the pathophysiology of thyroid carcinomas (10). Recently, there have been two reports of the mRNA expression of RXR isoforms in human thyroid carcinomas and matched normal thyroid tissues (28, 29). Tang *et al.* (28) have described a loss of mRNA expression observed in 18 cases for RAR- $\beta$ , six cases for RXR- $\alpha$ , and five cases for RXR- $\beta$ . In the same study, RAR- $\gamma$  and RXR- $\gamma$  were

expressed in all 42 paired normal thyroid and PTC samples examined (28). Haugen *et al.* (29) have found lower RAR- $\beta$ mRNA levels in seven of eight malignant thyroid tumors than in matched normal tissue. In contrast to Tang *et al.*, Haugen *et al.* (29) observed that RXR- $\gamma$  mRNA is not expressed in normal thyroid tissue but is highly expressed in subsets of human thyroid carcinoma tissues and cell lines. We also observed the decreased expression of mRNA in five of the six PTCs for RXR- $\alpha$  and RXR- $\beta$  and in four of the six PTCs for RXR- $\gamma$  (Fig. 4B). These controversial results might be explained by the design of the primers, the efficiency of PCR amplification, or unknown methodological factors.

Cytoplasmic staining was unexpectedly observed in some thyroid carcinomas with the use of the anti-RXR- $\alpha$  antibody (Fig. 1 and Fig. 2, A and G). Moreover, Western blot analysis showed that a novel RXR- $\alpha$ -related protein was expressed in the CEs from PTCs, MTCs, and FTCs (Fig. 1 and Fig. 5, B-D). Some previous studies have identified RXR- $\alpha$ -related proteins similar in molecular size to those seen in our study (16-18, 30-32). Matsushima-Nishiwaki *et al.* (16) have reported that calpain cleaves RXR- $\alpha$  into two fragments with molecular masses of 47 and 44 kDa; each

fragment was found to lack a portion of the N-terminal A/B domain in the NE of human hepatoma-derived HuH 7 cells. Furthermore, Nomura *et al.* (17) have indicated that cathepsin L-type protease in cytoplasm cleaves RXR- $\alpha$  into smaller fragments with molecular masses of 45, 43, and 31 kDa in two human-derived cell lines, HepG2 and JEG-3. They speculated that the 45- and 43-kDa fragments would lack the N-terminal A/B domain and that a fragment of 31 kDa would lack domains A through D of RXR- $\alpha$  (17). Our present findings were consistent with their results regarding the sizes of the RXR- $\alpha$ -related proteins. However, the results of Western blot analysis using two specific anti-RXR- $\alpha$  antibodies led us to speculate that the approximately 44-kDa protein lacked the C terminus of RXR- $\alpha$ , which might be a novel fragment of human RXR- $\alpha$  protein.

Previously, Blanco *et al.* (33) have shown that deletion of the C-terminal region converts RXR- $\alpha$  and RXR- $\beta$  to powerful dominant negative receptors that inhibit retinoic acid and Vitamin D-dependent transcription by respective heterodimer partners. Similarly, homozygous mutant mice expressing a truncated RXR- $\alpha$  (RXR- $\alpha$  AF2<sup>0</sup>) lacking C-terminal 18 amino acids, which includes the last helical  $\alpha$  structure of the

ligand-binding domain and the core of the activating domain of the activation function 2 of RXR- $\alpha$  protein, exhibit a subset of abnormalities (34) previously observed in RXR- $\alpha$ <sup>-/-</sup> mutants (35). These results suggested that the truncated RXR- $\alpha$  protein could not possess transcriptional activity because, in addition to its cytoplasmic localization, it lacked part of (or changed the conformation of) the ligand-binding domain, including activation function, which cannot be recognized by the anti-RXR- $\alpha$  antibody ( $\Delta$ DN197; Fig.5, C and D). Because of the interesting effects of RXR- $\alpha$ , we wish to gain some additional understanding of the function of this novel truncated protein.

The proteolytic fragment of RXR- $\alpha$  in the cytosol was produced, resulting in the translocation of RXR- $\alpha$  from the nucleus to the cytoplasm. Katagiri *et al.* (36) have demonstrated that nerve growth factor induces the phosphorylation of Ser 105 of nerve growth factor-induced clone B (NGFI-B) in PC 12 pheochromocytoma cells, increasing the export of the NGFI-B-RXR heterodimer complex from the nucleus to the cytoplasm. Recently, a nuclear localization sequence (NLS) of RXR was identified in the DNA-binding domain of RXR- $\alpha$  (37). Mutations in this NLS caused predominant cytoplasmic localization of *nls*YFP-RXR and prevented transcriptional activity (37).

Future work will also clarify whether or not the phosphorylation of heterodimerizing nuclear hormone receptors (*e.g.* TR, RAR, PPAR- $\gamma$ , and vitamin D<sub>3</sub> receptor) and/or the mutations in NLS of RXR- $\alpha$  regulates the subcellular distribution of RXR- $\alpha$  in thyroid carcinomas.

Retinoids have been administered as anticancer and preventive cancer treatments in various clinical trials, and previous studies of the effects of retinoids on thyroid cancer have demonstrated that they promote cell differentiation and regulate cellular proliferation (38-45). Recently, two clinical studies evaluated the redifferentiation effects of retinoic acids on thyroid cancer (46, 47). Simon *et al.* (46) have reported observing increased iodide uptake in 21 patients (42%). On the other hand, Gruning *et al.* (47) have found some improvement in radioiodine uptake in five (20%) of 25 patients, concluding that the therapeutic effects of retinoic acid in thyroid cancer are less than previously reported. Reduced expression of RXRs in human thyroid tumors, as demonstrated in the present study, could conceivably interfere with the inhibitory actions of retinoids on DNA synthesis and may thereby contribute to the development of thyroid carcinomas. Our present data, in combination with these earlier

results, lead us to propose the predictive parameters of successful redifferentiation therapy using retinoids on thyroid carcinomas.

### **Acknowledgements**

We are grateful to Mr. Toshimichi Fujisawa (Surgical Pathology, Ito Hospital) for help in preparation of the thyroid sections. We thank Mr. Masatoshi Sado (Surgical Pathology, Asahikawa Medical College) and Ms. Rie Matsumoto (The Second Department of Pathology, Asahikawa Medical College) for technical assistance of immunohistochemistry. We also thank Mr. Shinichi Chiba (Asahikawa Medical College) for technical assistance of a LightCycler. Dr. Naoko Sanno (Nippon Medical School, Tokyo, Japan) is thanked for technical advice on immunohistochemistry. We particularly acknowledge Dr. Akira Takeshita (Toranomon Hospital, Tokyo, Japan) for stimulating the initiation and progress of this study.

## References

1. **Hong WK, ItriLM** 1994 Retinoids and human cancer. In *The Retinoids; Biology, Chemistry, and Medicine* (2nd ed.), Sporn MB, Roberts AB, Goodman DS, editors. New York, Raven, 597-660
2. **Miyauchi J** 1999 All-trans retinoic acid and hematopoietic growth factors regulating the growth and differentiation of blast progenitors in acute promyelocytic leukemia. *Leuk Lymphoma* 33:267-280
3. **Fenaux P, Chomienne C, Degos L** 2001 All-trans retinoic acid and chemotherapy in the treatment of acute promyelocytic leukemia. *Semin Hematol.* 38:13-25
4. **Verma AK** 1987 Inhibition of both stage I and stage II skin tumor promotion by retinoic acid and the dependence of inhibition of tumor promotion on the duration of retinoic acid treatment. *Cancer Res* 47:5097-5101
5. **Lippmann SM, Meyskens Jr FL** 1987 Treatment of advanced squamous cell carcinoma of the skin with isotretinoin. *Ann Intern Med* 107: 499- 502
6. **Schmutzler C, Kohrle J** 2000 Retinoic acid redifferentiation therapy for thyroid

- cancer. *Thyroid* 10:393-406
7. **Chambon P** 1994 The retinoid signaling pathway: molecular and genetic analyses. *Semin Cell Biol* 5:115-125
  8. **Puzianowska-Kuznicha M, Krystyniak A, Madej A, Cheng SY, Nauman J** 2002 Functionally impaired TR mutants are present in thyroid papillary cancer. *J Clin Endocrinol Metab* 87:1120-1128
  9. **Kroll TG, Sarraf P, Pecciarini L, Chen CJ, Mueller E, Spiegelman BM, Fletcher JA** 2000 PAX8-PPAR $\gamma$ 1 fusion oncogene in human thyroid carcinoma. *Science* 289: 1357-1360
  10. **Schmutzler C, Brtko J, Winzer R, Jakobs TC, Meissner-Weigl J, Simon D, Goretzki PE, Kohrle J** 1998 Functional retinoid and thyroid hormone receptors in human thyroid cell lines and tissues. *Int J Cancer* 76:368-376
  11. **Sugawara A, Yen PM, Qi Y, Lechan RM, Chin WW** 1995 Isoform-specific retinoid X receptor (RXR) antibodies detect differential expression of RXR proteins in the pituitary gland. *Endocrinology* 136:1766-1774
  12. **Oikawa K, Kimura S, Aoki N, Atsuta Y, Takiyama Y, Nagato T, Yanai M,**

- Kobayashi H, Sato K, Sasajima T, Tateno M** 2004 Neuronal calcium sensor protein Visinin-like protein-3 interacts with microsomal cytochrome b5 in a  $\text{Ca}^{2+}$ -dependent manner. *J Biol Chem* 279: 15142-15152
13. **Pfaffl MW** 2001 A new mathematical model for relative quantification in real-time RT-PCR. *Nucleic Acid Res* 29:2002-2007
14. **Braun KW, Tribley WA, Griswold MD, Kim KH** 2000 Follicle-stimulating hormone inhibits all-trans-retinoic acid-induced retinoic acid receptor  $\alpha$  nuclear localization and transcriptional activation in mouse sertoli cell lines. *J Biol Chem* 275:4145-4151
15. **Haugen BR, Brown NS, Wood WM, Gordon DF, Ridgway EC** 1997 The thyrotrope-restricted isoform of the retinoid-X receptor- $\gamma$ 1 mediates 9-cis-retinoic acid suppression of thyrotropin- $\beta$  promoter activity. *Mol Endocrinol* 11:481-489
16. **Matsushima-Nishiwaki R, Shindoji Y, Nishiwaki S, Moriwaki H, Muto Y** 1996 Limited degradation of retinoid X receptor by calpain. *Biochem Biophys Res Commun* 225:946-951

17. **Nomura Y, Nagaya T, Yamaguchi S, Katunuma N, Seo H** 1999 Cleavage of RXR $\alpha$  by a Lysosomal Enzyme, Cathepsin L-type protease. *Biochem Biophys Res Commun* 254:388-394
18. **Pruffer K, Schroder C, Hegyi K, Barsony J** 2002 Degradation of RXRs influences sensitivity of rat osteosarcoma cells to the antiproliferative effects of calcitriol. *Mol Endocrinol* 16:961-976, 2002
19. **Mangelsdorf DJ, Ong ES, Dyck JA, Evans RM** 1990 Nuclear receptor that identifies a novel retinoic acid response pathway. *Nature* 345:224-229
20. **Yu VC, Delsert C, Andersen B, Holloway JM, Devary OV, Naar AM, Kin SY, Boutin J-M, Glass CK, Rosenfeld MG** 1991 RXR $\beta$ : a coregulator that enhances binding of retinoic acid, thyroid hormone, and vitamin D receptors to their cognate response elements. *Cell* 67:1251-1266
21. **Mangelsdorf DJ, Hallenbeck PL, Nagata T, Segars JH, Appella E, Nikodem VM, Ozato K** 1992 H-2RIIBP (RXR $\beta$ ) heterodimerization provides a mechanism for combination diversity in the regulation of retinoic acid and thyroid hormone responsive genes. *EMBO J* 11:1419-1435

22. **Mano H, Ozawa T, Takeyama K, Yoshizawa Y, Kojima R, Kato S, Masushige S** 1993 Thyroid hormone affects the gene expression of retinoid X receptors in the adult rat. *Biochem Biophys Res Commun* 191:943-949
23. **Dolle P, Fraulob V, Kastner P, Chambon P** 1994 Developmental expression of murine retinoid X receptor (RXR) genes. *Mech Dev* 45:91-104
24. **Moreno S, Farioli-Vecchioli S, Ceru MP** 2004 Immunolocalization of peroxisome proliferator activated receptors and retinoid X receptors in the adult rat CNS. *Neuroscience* 123:131-145
25. **Liu Q, Linney E** 1993 The mouse retinoid-X receptor- $\gamma$  gene: genomic organization and evidence for functional isoforms. *Mol Endocrinol* 7:651-658
26. **Sanno N, Sugawara A, Teramoto A, Abe Y, Yen PM, Chin WW, Osamura RY** 1997 Immunohistochemical expression of retinoid X receptor isoforms in human pituitaries and pituitary adenomas. *Neuroendocrinology* 65:299-306
27. **Brown NS, Smart A, Sharma V, Brinkmeier ML, Greenlee L, Camper SA, Jensen DR, Eckel RH, Krezel W, Chambon P, Haugen BR** 2000 Thyroid hormone resistance and increased metabolic rate in the RXR- $\gamma$ -deficient mouse.

J Clin Invest 106:73-79

28. **Tang W, Nakamura Y, Zuo H, Yasuoka H, Yang Q, Wang X, Nakamura M, Mori I, Miyauchi A, Kakudo K** 2003 Differentiation, proliferation and retinoid receptor status of papillary carcinoma of the thyroid. *Pathol Int* 53:204-213
29. **Haugen BR, Larson LL, Pugazhenti U, Hays WR, Klopper JP, Kramer CA, Sharma V** 2004 Retinoic acid and retinoid X receptors are differentially expressed in thyroid cancer and thyroid carcinoma cell lines and predict response to treatment with retinoids. *J Clin Endocrinol Metab* 89:272-280
30. **Nagaya T, Murata Y, Yamaguchi S, Nomura Y, Ohmori S, Fujieda M, Katunuma N, Yen PM, Chin WW, Seo H** 1998 Intracellular proteolytic cleavage of 9-cis-retinoic acid receptor  $\alpha$  by cathepsin L-type protease is a potential mechanism for modulating thyroid hormone action. *J Biol Chem* 273:33166-33173
31. **Matsushima-Nishiwaki R, Okuno M, Sano T, Akita K, Moriwaki H, Friedman SL, Kojima S** 2001 Phosphorylation of retinoid X receptor  $\alpha$  at serine 260 impairs its metabolism and function in human hepatocellular

- carcinoma. *Cancer Res* 61:7675-7682
32. **Casas F, Daury L, Grandemange S, Busson M, Seyer P, Hatier R, Caraso A, Cabello G, Wrutniak-Cabello C** 2003 Endocrine regulation of mitochondrial activity: involvement of truncated RXR $\alpha$  and c-Erb A $\alpha$ 1 proteins. *FASEB J* 17:426-436
33. **Blanco JC, Dey A, Leid M, Minucci S, Park BK, Jurutka PW, Haussler MR, Ozato K** 1996 Inhibition of ligand induced promoter occupancy in vivo by a dominant negative RXR. *Gene Cells* 1:209-221
34. **Mascrez B, Mark M, Dierich A, Ghyselinck NB, Kastner P, Chambon P** 1998 The RXR $\alpha$  ligand-dependent activation function (AF-2) is important for mouse development. *Development* 125:4691-4707
35. **Kastner P, Grondona JM, Mark M, Gransmuller A, Le Meur M, Decimo D, Vonesch JL, Dolle P, Chambon P** 1994 Genetic analysis of RXR $\alpha$  developmental function: convergence of RXR and RAR signaling pathways in heart and eye morphogenesis. *Cell* 78:987-1003
36. **Katagiri Y, Takeda K, Yu Zu-Xi, Ferrans VJ, Ozato K, Guroff G** 2000

- Modulation of retinoid signaling through NGF-induced nuclear export of NGFI-B. *Nature Cell Biology* 2:435-440
37. **Prufer K, Barsony J** 2002 Retinoid X receptor dominates the nuclear import and export of the unliganded Vitamin D receptor. *Mol Endocrinol* 16:1738-1751
38. **Del Senno L, Rossi R, Gandini D, Piva R, Franceschetti P, Degli Uberti EC** 1993 Retinoic acid induced decrease of DNA synthesis and peroxidase mRNA levels in human thyroid cells expressing retinoic acid receptor alpha mRNA. *Life Sci* 53:1039-1048
39. **Van Herle AJ, Agatep ML, Padua DN 3rd, Totanes TL, Canlapan DV, Van Herle HM, Juillard GJ** 1990 Effects of 13 cis-retinoic acid on growth and differentiation of human follicular carcinoma cells (UCLA R0 82 W-1) in vitro. *J Clin Endocrinol Metab* 71:755-63
40. **Arai M, Tsushima T, Isozaki O, Shizume K, Emoto N, Demura H, Miyakawa M, Onoda N** 1991 Effects of retinoids on iodine metabolism thyroid peroxidase gene expression, and deoxyribonucleic acid synthesis in porcine thyroid cells in culture. *Endocrinology* 129:2827-2833

41. **Namba H, Yamashita S, Morita S, Villadolid MC, Kimura H, Yokohama N, Izumi M, Ishikawa N, Ito K, Nagataki S** 1993 Retinoic acid inhibits in human thyroid peroxidase and thyroglobulin gene expression in cultured human thyrocytes. *J Endocrinol Invest* 16:87-93
42. **Schreck R, Schnieders F, Shmutzler C, Kohrle J** 1994 Retinoids stimulate type I iodothronine 5'-deiodinase activity in human follicular thyroid carcinoma cell lines. *J Clin Endocrinol Metab* 79:791-798
43. **Paez Pereda M, Missale C, Grubler Y, Arzt E, Schaaf L, Stalla GK** 2000 Nerve growth factor and retinoic acid inhibit proliferation and invasion in thyroid tumor cells. *Mol Cell Endocrinol* 167:99-106
44. **Havekes B, Schroder van der Elst JP, van der Pluijm G, Goslings BM, Morreau J, Romijin JA, Smit JWA** 2000 Beneficial effects of retinoic acid on extracellular matrix degradation and attachment behavior in follicular thyroid carcinoma cell lines. *J Endocrinol* 167:229-23.
45. **Kurebayashi J, Tanaka K, Otsuki T, Moriya T, Kunisue H, Uno M, Sonoo H** 2000 All-trans-retinoic acid modulates expression levels of thyroglobulin and

- cytokines in a new human poorly differentiated papillary thyroid carcinoma cell line, KTC-1. J Clin Endocrinol Metab 85: 2889-2896
46. **Simon D, Korber C, Krausch M, Segering J, Groth P, Grunwald F, Muller-Gartner HW, Schmutaler C, Kohrle J, Roher HD, Reiners C** 2002  
Clinical impact of retinoids in redifferentiation therapy of advanced thyroid cancer; final results of a pilot study. Eur J Nucl Med 29:775-782
47. **Gruning T, Tiepolt C, Zophel K, Bredow J, Kropp J, Franke WG** 2003  
Retinoic acid for redifferentiation of thyroid cancer-does it hold its promise?  
Eur J Endocrinol 148:395-402

### Figure Legends.

#### **Figure 1. Western blot analysis and immunohistochemistry of the PTC.**

Immunopositive cells appear brown as a result of DAB colorimetric reaction (*top*).

Each anti-RXR isoforms antibody detected the strong (level=3) or moderate (level=2)

nuclear staining in normal thyroid tissue (*arrow*) and absent (level=0) nuclear staining

in PTC (*arrowhead*). Normal thyroid is at left. Samples (standardized to 20 µg of total

protein/lane) were size-separated on a 4-12 % NuPage bis-Tris SDS-PAGE gels and

transferred to an Immobilon-P membrane. After blocking with 5 % nonfat dry milk, the

blot was incubated with the rabbit antihuman RXR isoforms and then stained with

secondary antibody-linked horseradish peroxidase. Size standards are shown at the *left*.

Lane 1, NE from normal thyroid tissue; lane 2, NE from PTC; lane 3, CE from normal

thyroid tissue; lane 4, CE from PTC. Appropriately sized protein bands in NEs from

normal thyroid tissues were demonstrated for each RXR isoform (*bottom*, lane 1, *arrow*).

The two immunoreactive bands in NE from normal thyroid tissue were detected by

anti-RXR- $\gamma$  antibody (*bottom right*). The CE from PTC, which showed the strong

cytoplasmic immunostaining for RXR- $\alpha$ , showed strong reaction at a molecular mass

of approximately 44 kDa by anti-RXR- $\alpha$  antibody (D-20) (*asterisk*).

**Figure 2. Representative staining of RXR isoforms in thyroid carcinomas and normal (N) surrounding thyroid tissue.** Immunopositive cells appear *brown* as a result of 3,3'-diaminobenzidine tetrahydrochloride colorimetric reaction. A, PTC. Normal thyroid is at *lower right*. RXR- $\alpha$  demonstrated strong (level = 3) to moderate (level = 2) nuclear staining in adjacent normal thyroid follicular cells. In contrast, moderate (level = 2) cytoplasmic staining was observed in PTC cells by anti-RXR- $\alpha$  antibody (D-20; original magnification, x200). The *inset* shows the higher magnification of PTC (original magnification, x400). The strong granular staining was seen in the cytoplasm in PTC. C, FTC cells protrude into a vessel in its capsule. Normal thyroid is at *bottom*. FTC demonstrated moderate (level = 2) nuclear staining with absent (level = 0) cytoplasmic staining of RXR- $\beta$  (magnification, x200). E, MTC. Normal thyroid is at *left*. MTC shows almost absent (level = 0) nuclear immunostaining of RXR- $\gamma$ , whereas surrounding normal thyroid follicular cells indicated the strong (level = 3) nuclear staining (magnification, x200). *Inset* is the higher magnification of normal thyroid cells

(original magnification, x400). G, Large-cell ATC with a lymphocytic reaction. ATC demonstrated absent (level = 0) nuclear staining with moderate (level = 2) and granular cytoplasmic staining of RXR- $\alpha$  (magnification, x200). H, FA had a thick capsule and displayed strong (level = 3) nuclear immunoreactivity for RXR- $\alpha$  (magnification, x200). B, D, and F, The positive staining appears specific by immunocytochemical criteria because each blocking peptide completely blocked the staining (magnification, x200).

**Figure 3. Distribution of RXR isoforms immunostaining intensity in nucleus and cytoplasm in thyroid samples (57 PTCs, 40 FTCs, 24 ATCs, 28 MTCs and 27 FAs).**

The intensity of staining of tumors was compared to that of normal thyroid follicular cells in the margin of each specimen. Because normal follicular thyroid cells showed moderate (level = 2) or strong (level = 3) nuclear staining accompanied with absent (level= 0) or weak (level =1) cytoplasmic staining, tumors were considered to have a suppressed nuclear RXR expression when the nuclear intensity level of the tumor cell was less than 2 (moderate); if the cytoplasmic staining level was higher than 2, a tumor was considered to have the increased cytoplasmic RXR expression. The y-axis

represents the percentage of cases in each histological category of tumor samples. *Open bars* showed absent (level = 0) or weak (level = 1) immunostaining for each RXR isoform, and *filled bars* showed moderate (level = 2) or strong (level = 3) staining for each RXR isoform. For comparative analysis, two-tailed Fisher's exact test was used to compare the differences in the expression of the RXR isoforms between two histological types.  $P < 0.05$  was accepted as statistically significant. \*\*,  $P < 0.01$ , \*,  $P < 0.05$ .

**Figure 4. A. RXR $\alpha$  transcripts detected by RT-PCR in paired normal thyroid tissue and PTC.** To evaluate the possibility that PTC showing cytoplasmic immunostaining for RXR- $\alpha$  protein would also express different sizes of mRNA, we performed RT-PCR by using the mRNA extracted from the normal thyroid tissue and PTC. There was no different sized band seen in both samples. Marker, 1 kb DNA ladder (Invitogen). **B. Relative quantification of RXR mRNA expression in representative PTCs, FTC, MTC and FA.** Real-time PCR was performed using a LightCycler system. The single cDNA obtained by reverse transcription from tissues

was used as a template for real-time PCR. Each histogram indicates the relative expression ratio. The control tissue is a surrounding normal thyroid tissue.  $\beta$ -actin was used as a reference gene. *Open bars* are the matched normal thyroid tissues, and *filled bars* are the tumor tissues.

**Figure 5. Western blot analysis of RXR- $\alpha$  in PTC, FTC, and MTC.** A, Structure of human RXR- $\alpha$  and epitopes of antibodies against RXR- $\alpha$ . RXR- $\alpha$  (A/B)(D-20): amino acid 2-21; RXR- $\alpha$  (E) ( $\Delta$ DN197): amino acids 198-462 (A/B, transactivation domain; C, DNA binding domain; D, hinge region; and E, ligand-binding domain). B, Western blot analysis of NEs and CEs from PTCs, which shows the moderate (level = 2) cytoplasmic immunostainings and the decreased nuclear immunostainings of RXR- $\alpha$  and surrounding normal thyroid tissues. N, Normal thyroid tissue; T, neoplastic lesions. Number indicates case number. C, Western blot analysis of NEs and CEs isolated from PTC (T) and surrounding normal tissue (N) using two specific RXR- $\alpha$  a (A/B) (D-20) or antihuman RXR- $\alpha$  (E) ( $\Delta$ DN197). D, Western blot analysis of MTCs and FTCs. Number indicates case number. An *arrowhead* indicates the mobility of 54

kDa, and an *asterisk* indicates the mobility of 44 kDa.

**Figure 6. Expression of RXR isoforms in human thyroid cancer cell lines.** A, RXR isoform mRNA in thyroid carcinoma cell line. Total RNA extracted from human thyroid cancer cell lines ARO, WRO and NPA was reverse transcribed and amplified with specific primer, as described in *Materials and Methods* (Table 1). The size of each amplified cDNA is indicated.  $\beta$ -actin gene served as the internal control. B, Expression of RXR- $\alpha$  protein in human thyroid cancer cell lines. NEs and CEs from ARO, WRO and NPA cells were subjected to Western blot, and the membranes were incubated with antihuman RXR- $\alpha$  antibody (D-20). An *arrow* indicates the mobility of 54 kDa, and an *asterisk* indicates the mobility of 44 kDa.

**TABLE 1. Oligonucleotide sequences for RT-PCR amplification of mRNA species and nucleotide positions of oligonucleotides.**

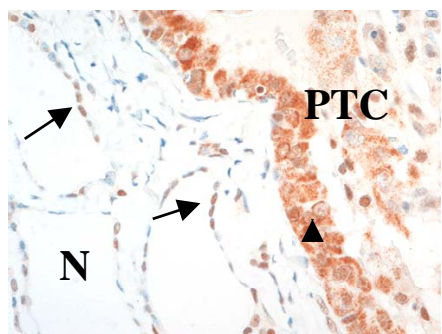
Target genes	Primer sequence (5'→ 3')	Nucleotide position	Annealing Temperature (°C)	No. of PCR cycles <sup>a</sup>	Expected size (bp)
RXR $\alpha$	Forward: TTCGCTAAGCTCTTGCTC Reverse: ATAAGGAAGGTGTCAATGGG	1318-1335 1430-1411	55	30	113
RXR $\beta$	Forward: GAAGCTCAGGAAACACTAC Reverse: TGCAGTCTTTGTTGTCCC	257-176 367-350	55	35	111
RXR $\gamma$	Forward: GAGGCTCCCCTGGCCACAC Reverse: GGTGCCTGAGACTCACGTC	74-92 202-184	55	35	129
$\beta$ -actin	Forward: ACCCACA CTGTGCCCATGTA Reverse: CGG AACCGCTCATTGCC	551-567 840-824	55	25	289

<sup>a</sup>Numbers of cycles were determined to amplify both products logarithmically and in relatively similar amounts.

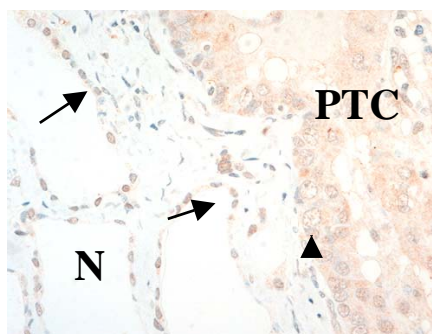


The relationship between the expression of each RXR isoform and the tumor type was analyzed by the Friedman test. The nuclear and cytoplasmic expression values of the isoforms were significantly decreased in all four classes of thyroid carcinomas ( $P < 0.05$ ), except for the cytoplasmic expression of RXR- $\alpha$  protein ( $P = 0.27$ ). However, there was only a specific correlation between nuclear RXR- $\gamma$  expression and histological typing of thyroid tumors ( $P = 0.04$ ), indicating a statistical difference between PTC and ATC in the nuclear expression of RXR- $\gamma$  ( $P < 0.05$ ).

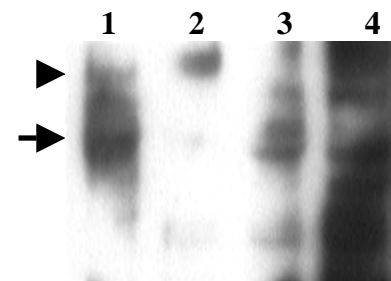
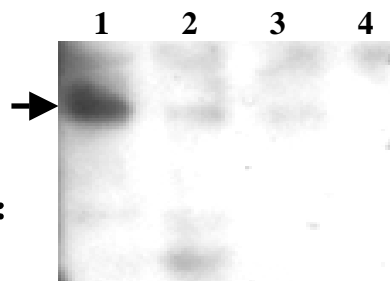
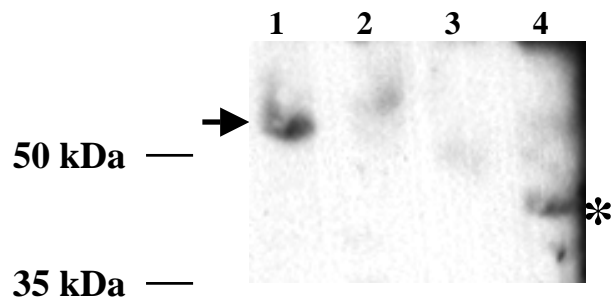
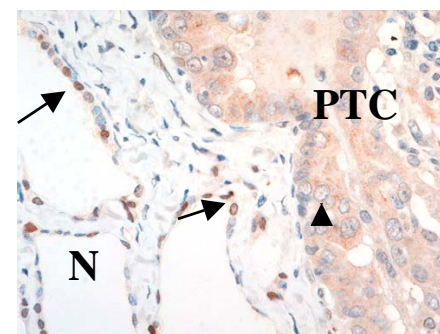
**RXR $\alpha$**

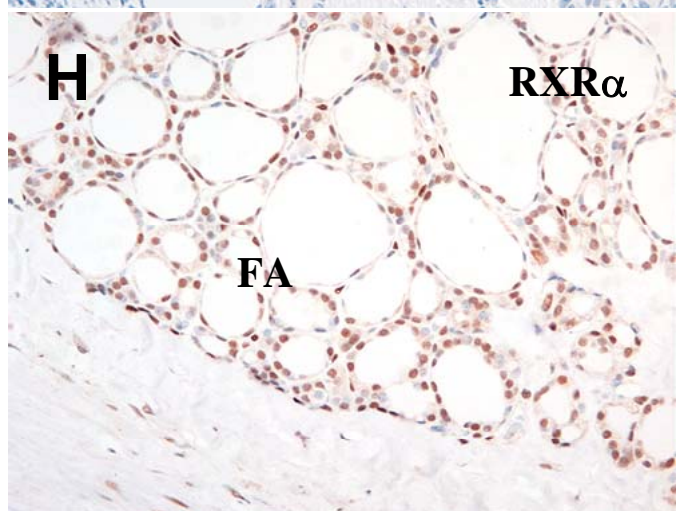
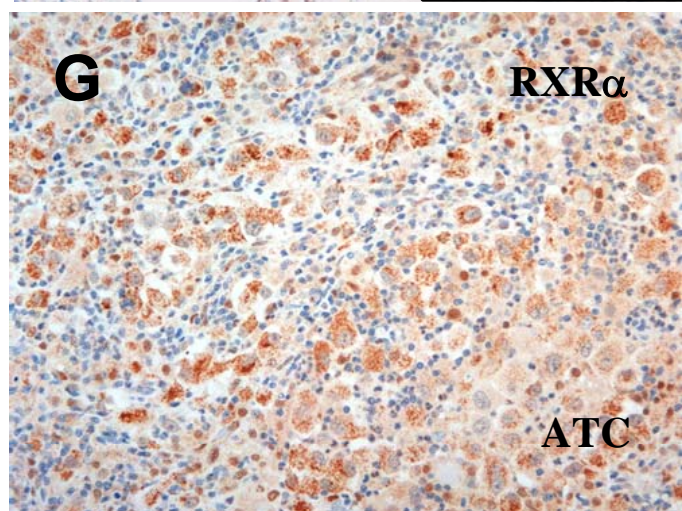
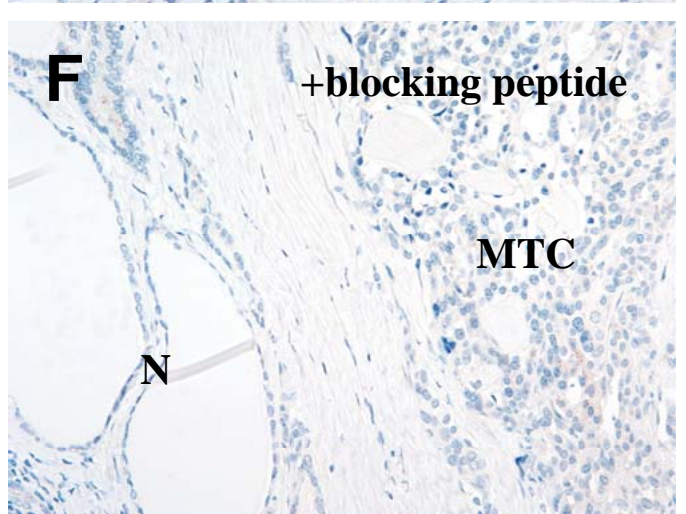
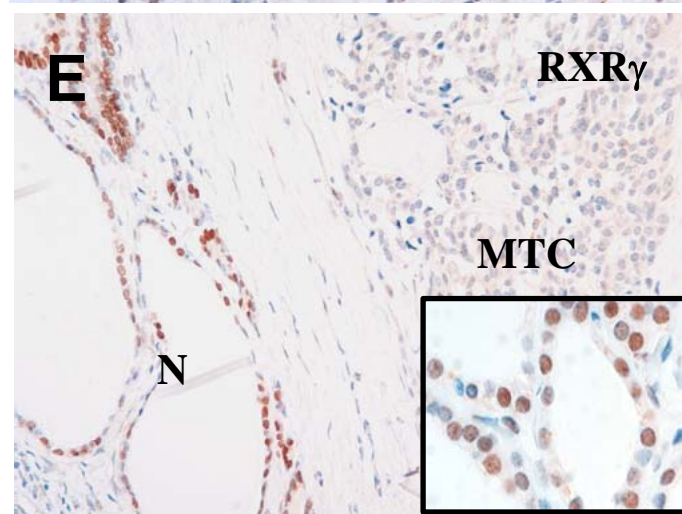
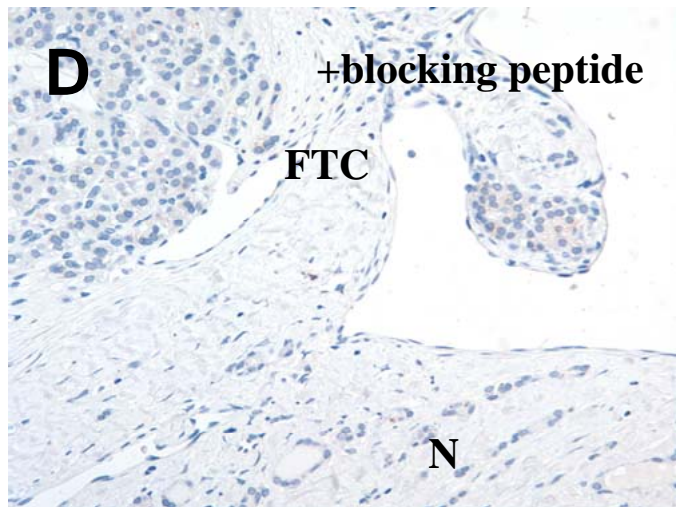
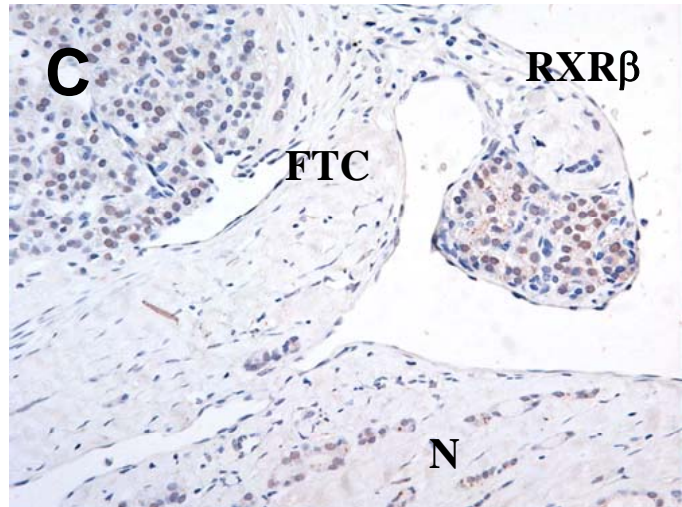
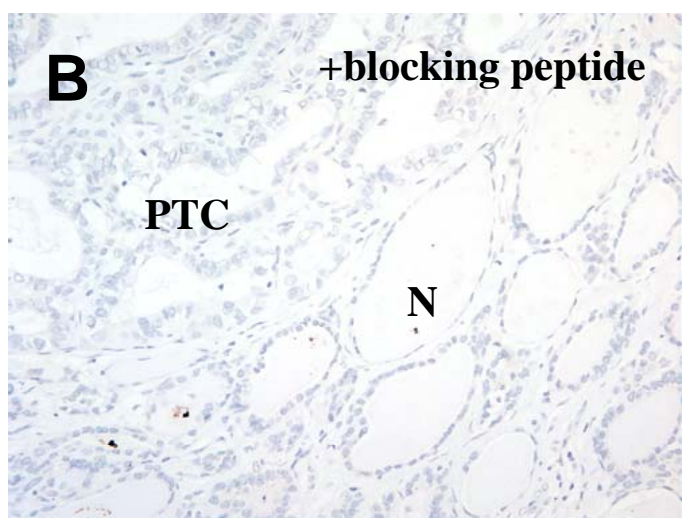
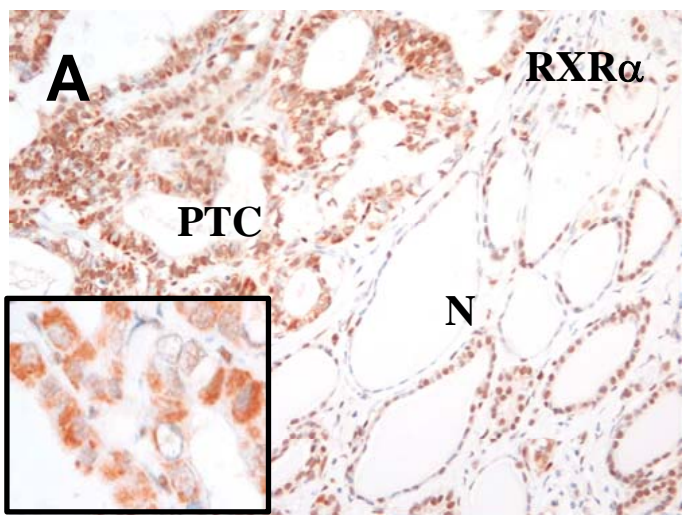


**RXR $\beta$**

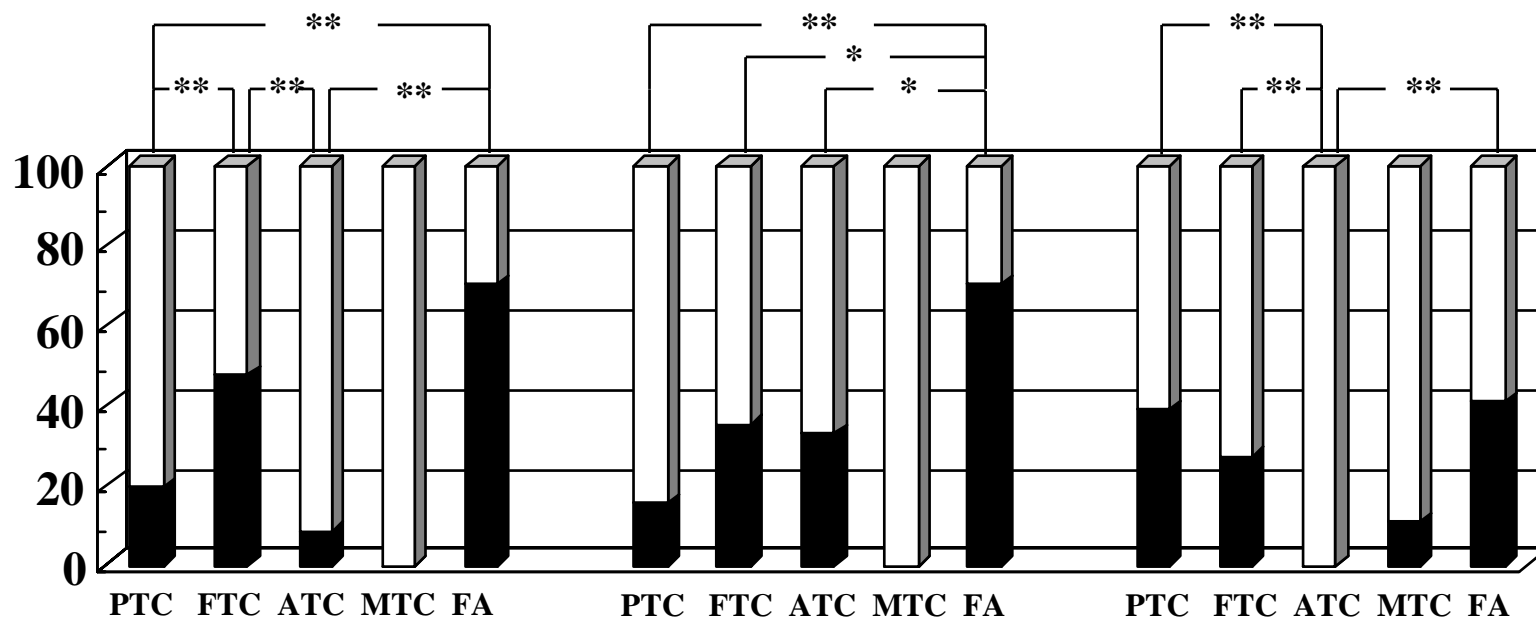


**RXR $\gamma$**

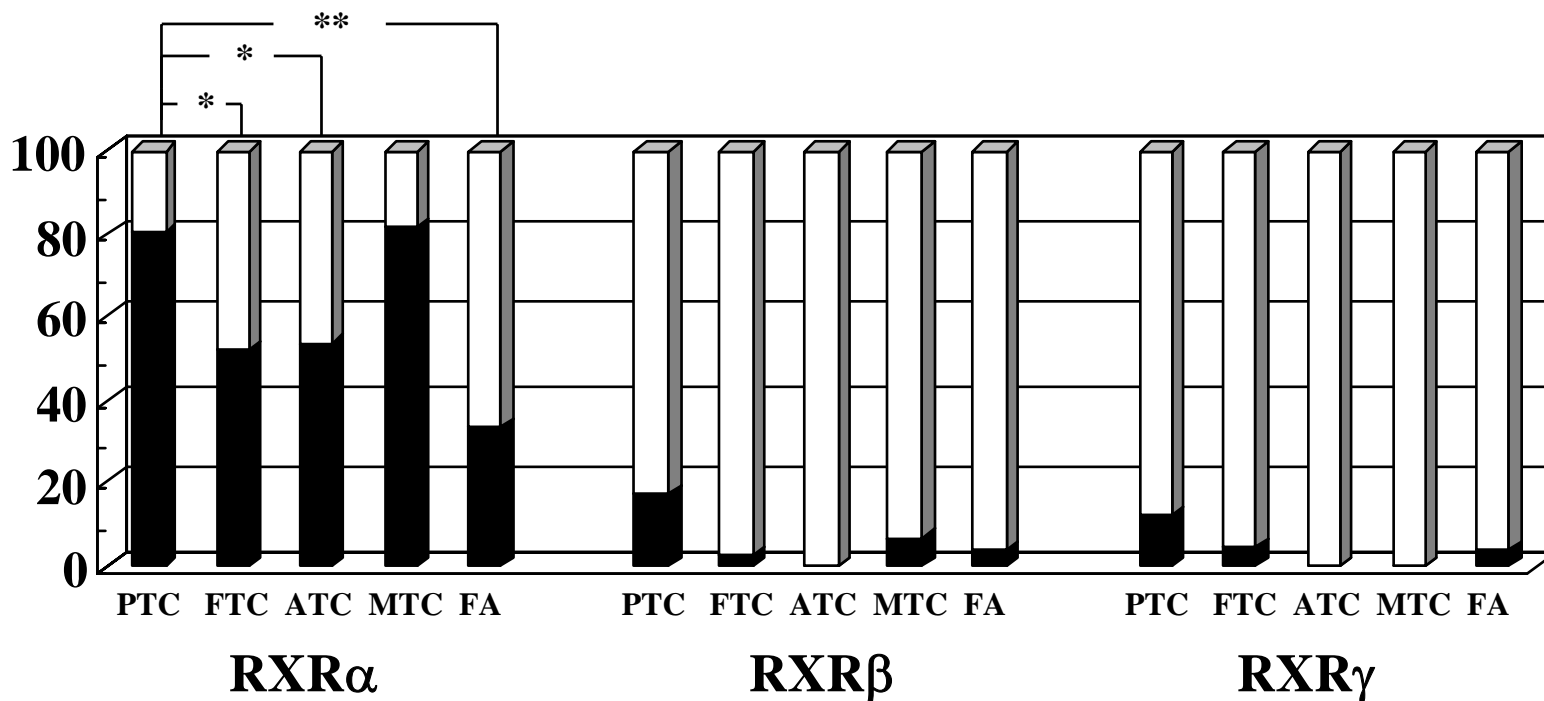




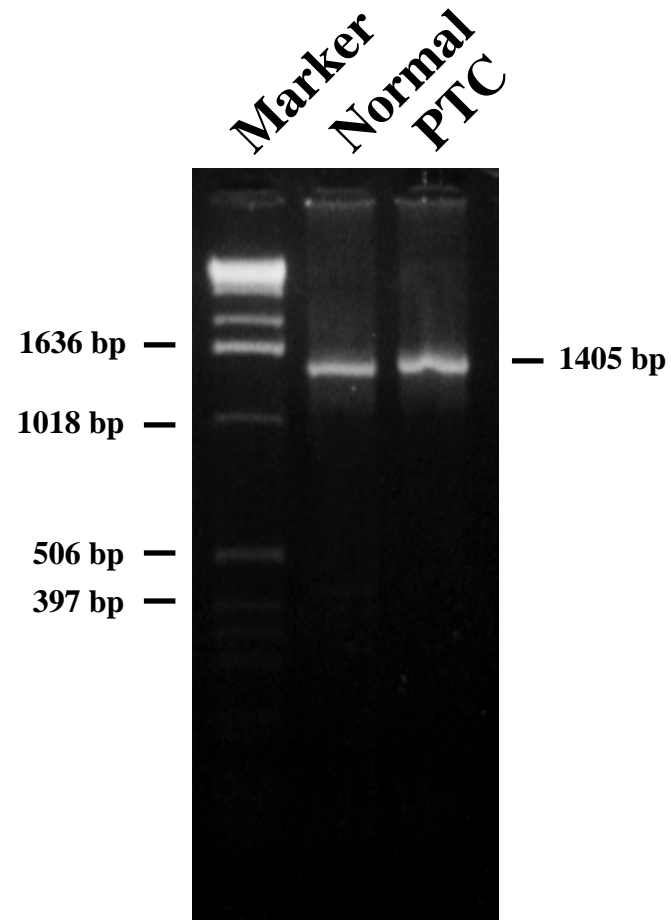
### Nuclear Staining

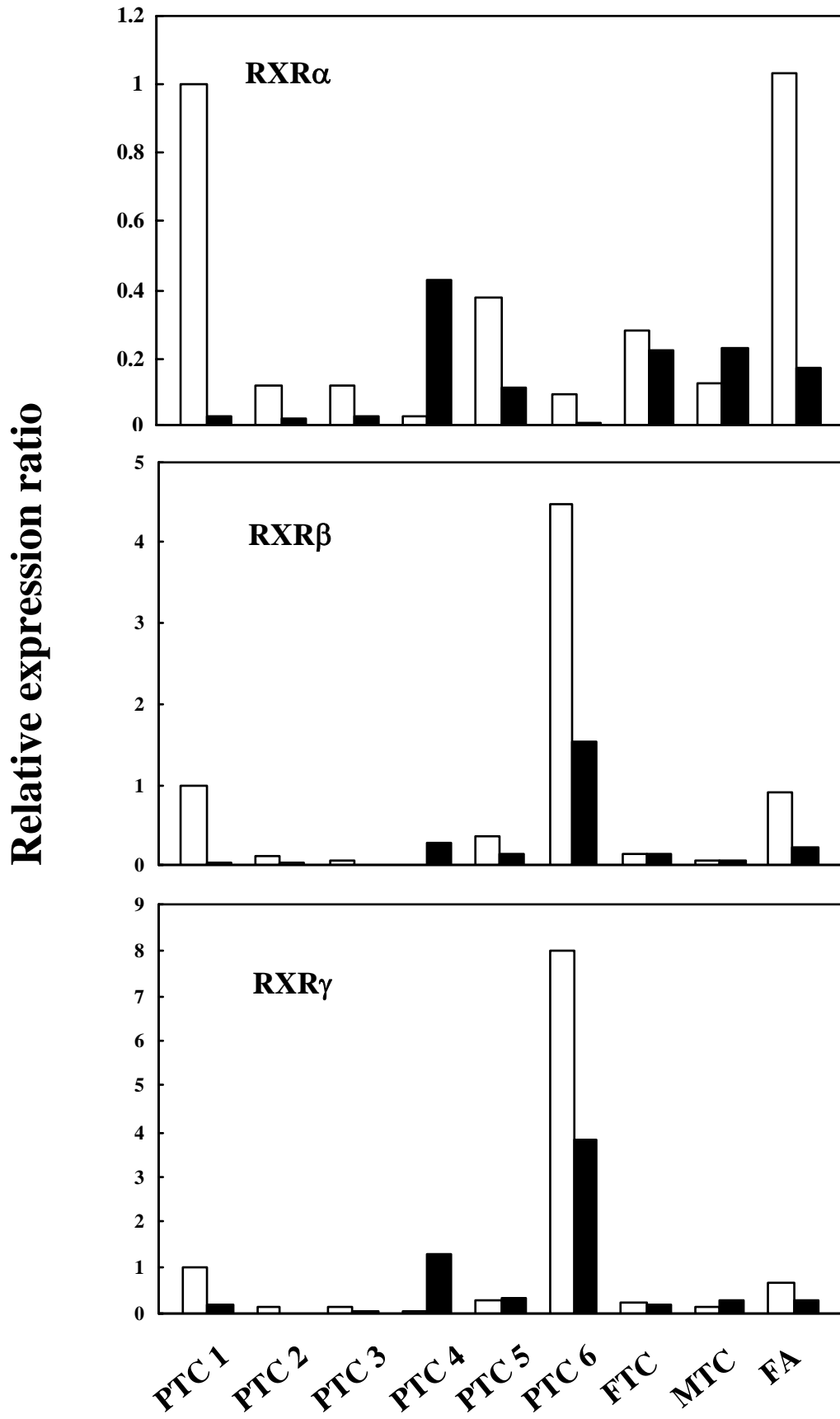


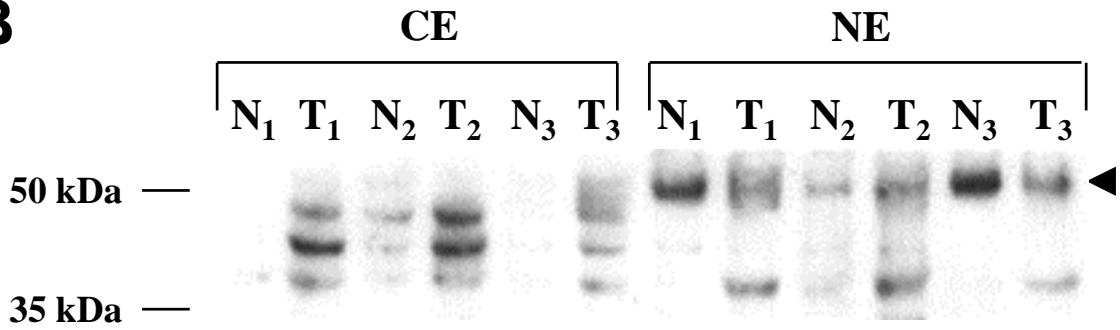
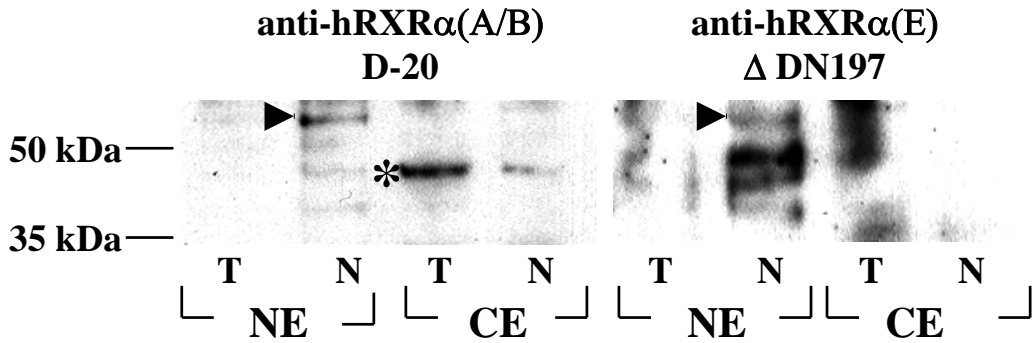
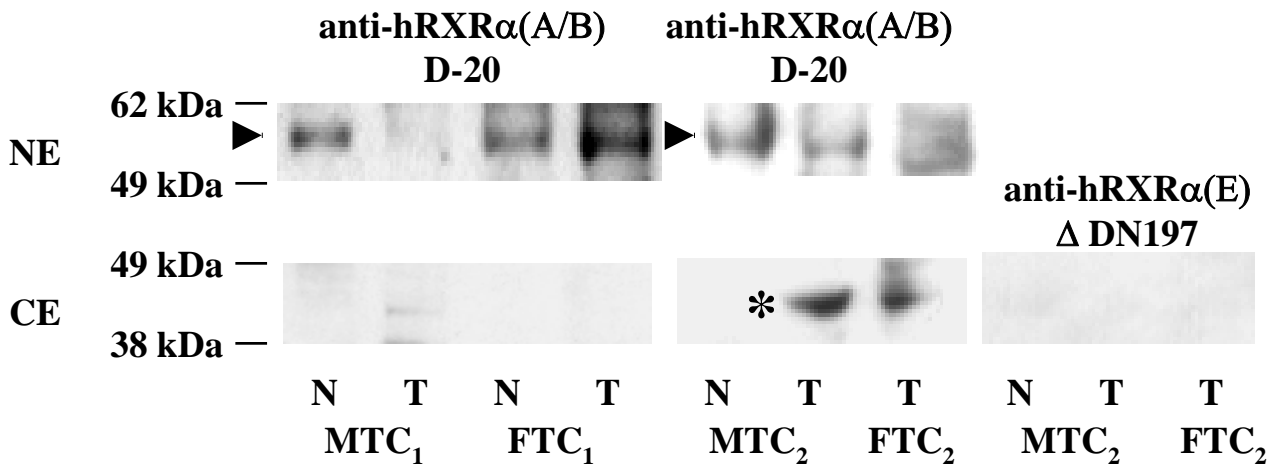
### Cytoplasmic Staining



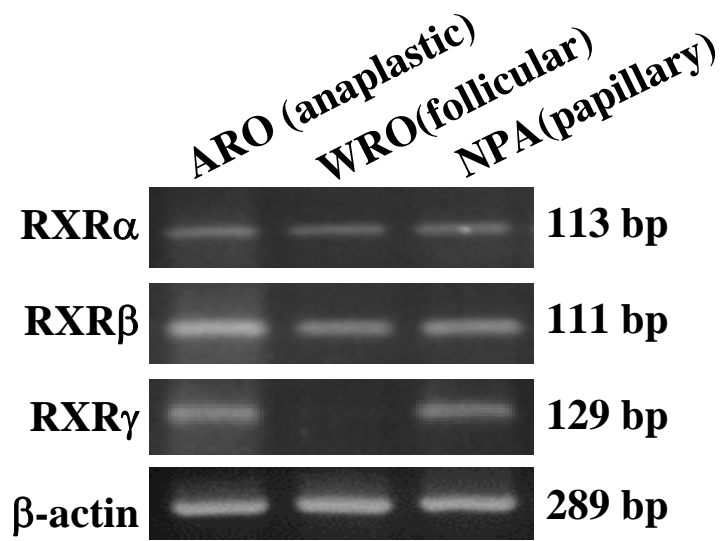
**A**



**B**

**A****B****C****D**

**A**



**B**

